Geothermics, Vol. 22, No. 3, pp. 151–163, 1993.
Printed in Great Britain.

Pergamon Press Ltd
CNR.

HEAT FLOW FROM FOUR NEW RESEARCH DRILL HOLES IN THE WESTERN CASCADES, OREGON, U.S.A.

S. E. INGEBRITSEN,* M. A. SCHOLL* and D. R. SHERROD†

**U.S. Geological Survey, 345 Middlefield Rd, Menlo Park, CA 94025, U.S.A. and †U.S. Geological Survey, Vancouver, Washington, U.S.A.*

(*Received January* 1993; *accepted for publication March* 1993)

Abstract—Conceptual models of the thermal structure of the Oregon Cascade Range propose either (1) a narrow zone of magmatic heat sources, flanked by shallow heat-flow anomalies caused by lateral ground-water flow; or (2) a wide zone of magmatic heat sources, with localized, generally negligible ground-water effects. The proposed narrow heat source coincides with the Quaternary volcanic arc, whereas the wider heat source would extend 10–30 km west of the arc. To test the models, four new heat-flow holes were sited west of the Quaternary arc but within the area of the proposed wide heat source. The sites are separated from the Quaternary arc by topographic divides and (or) major river valleys, so that heating by regional-scale ground-water flow seems unlikely. Measured heat flow (76 ± 5 mW m^{-2}) was significantly lower than the values predicted by interpolation from an existing heat-flow contour map (95 ± 7 mW m^{-2}). The lower values are consistent with a narrow zone of magmatic heat sources. The complete heat-flow data set consists mostly of shallow (100–200 m) data and defines lobate highs around hot-spring groups in the Western Cascades. However, all of the deepest holes in the study area (44°–45°15′N) show hydrologic gradient disturbances extending to depths >200 m, so the shallow data must be extrapolated with caution.

Key words: heat flow ground water volcanoes thermal conductivity Cascade Range

INTRODUCTION

Conductive heat-flow data from the central Oregon Cascade Range indicate that the Quaternary volcanic arc and adjacent 2–7 Ma volcanic rocks constitute a large area of low-to-zero near-surface conductive heat flow, due to downward and lateral flow of cold ground water. In contrast, near-surface conductive heat flow is high (>100 mW m^{-2}) in rocks older than ~7 Ma exposed at lower elevations in the adjacent Western Cascades.

A broad, generally uneroded ridge of permeable Quaternary and upper Pliocene volcanic rocks known as the High Cascades forms the crest of the Cascade Range in central Oregon, U.S.A. The Western Cascades are a deeply incised terrain underlain by less permeable Oligocene–lower Pliocene volcanic and volcaniclastic rocks. The High Cascades receive heavy snowfall, and about half of the incident precipitation infiltrates and recharges local- and regional-scale ground-water systems (Ingebritsen *et al.*, 1991, 1992). Hot-spring systems that appear to be recharged in the High Cascades discharge significant amounts of heat in the deeply incised valleys of the Western Cascades. Between 44° and 45°15′N, the rate of advective heat transfer by hot-spring systems is ~0.9 MW per km arc length, though the length normalization is problematic, because the distribution of hot-spring heat discharge is very uneven (Ingebritsen *et al.*, 1989, 1991).

Alternative conceptual models for the deeper thermal structure have been developed to explain these shallow observations, and have significant implications for the nature of arc magmatism and associated geothermal-resource potential. The "lateral-flow" model (Fig. 1A) suggests a relatively narrow zone of magmatic heating essentially confined to the Quaternary arc and flanked by shallow-rooted heat-flow anomalies caused by regional ground-water flow. The

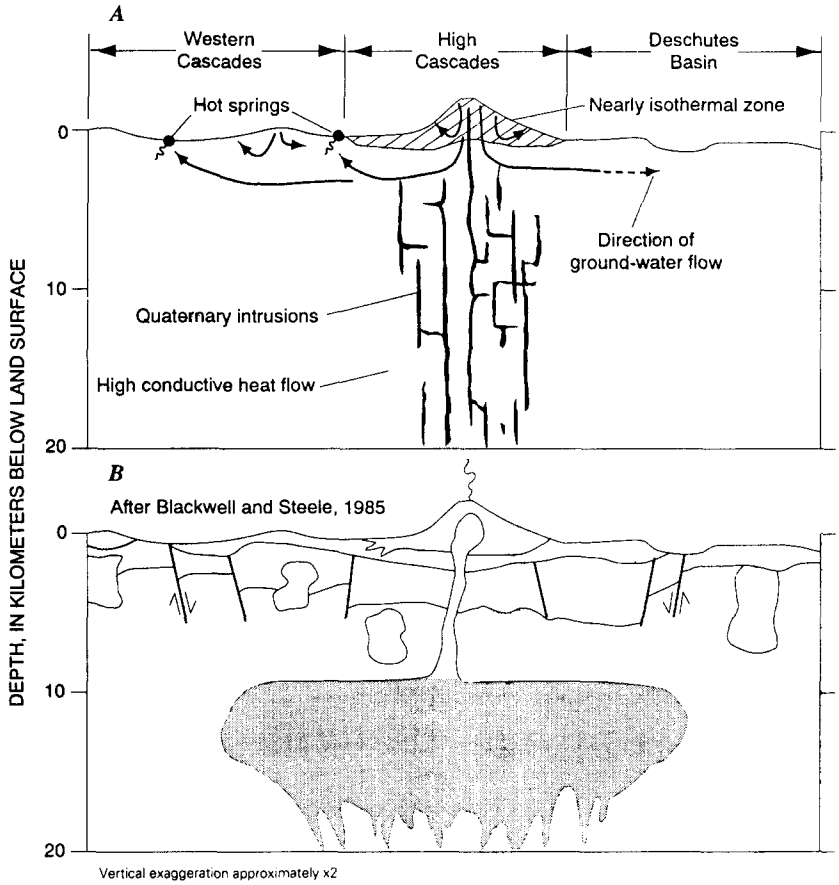

Fig. 1. Conceptual models of the thermal structure of the north-central Oregon Cascades, showing: (A) magmatic heat sources beneath the Quaternary arc ("lateral-flow" model); and (B) an extensive mid-crustal heat source.

"mid-crustal heat-source" model (Fig. 1B) suggests a laterally extensive zone of magmatic intrusion and heating that extends beneath adjacent parts of the older Western Cascades. These alternative conceptual models were discussed in detail by Blackwell *et al.* (1982, 1990b) and Ingebritsen *et al.* (1989, 1992).

Ingebritsen *et al.* (1991, 1992) simulated ground-water flow and heat transport through two cross-sections extending westward from the Cascade Range crest: one in the Breitenbush area, where there is no major arc-parallel normal faulting, and one in the McKenzie River area, where major graben-bounding faults exist (see Fig. 2 for locations of Breitenbush Hot Springs and McKenzie River). In the simulations, the alternative conceptual models were represented as wide or localized deep heat sources. Either model can satisfy the thermal observations. Data from the Breitenbush Hot Springs area seem to require significant advective heat transfer, whereas sparser observations in the McKenzie River area can be satisfied with either advection- or conduction-dominated simulations. Because of the large topographic gradient (~0.1), transmissivities of ~1 darcy m are sufficient to transfer ~1 MW per km arc length from the High Cascades to the Western Cascades. The Breitenbush observations can be explained in terms of lateral flow at ~1 km depth, but successful advection-dominated simulations of the McKenzie River section required ~1 darcy m transmissivities at depths of several kilometers, because

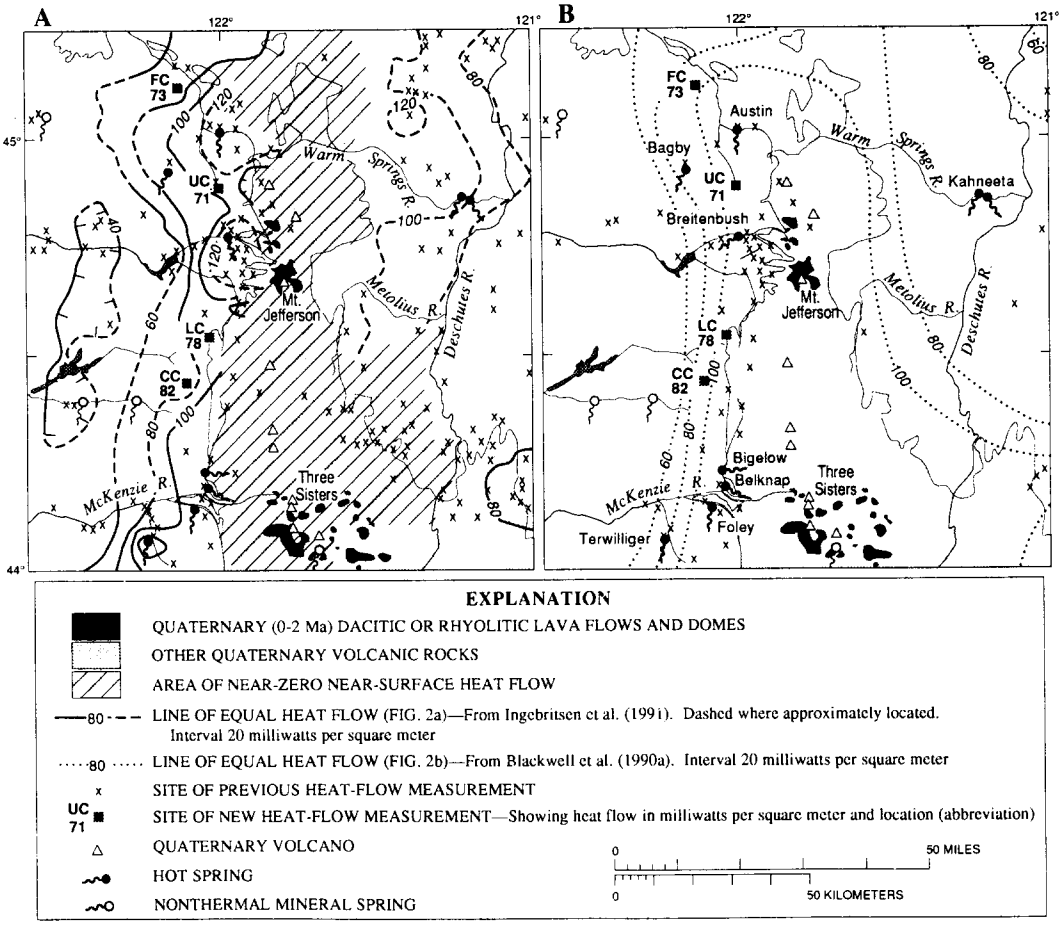

Fig. 2. Conductive heat-flow contours from: (A) Ingebritsen *et al.* (1991); and (B) Blackwell *et al.* (1990a). [Drill sites: FC = Fish Creek, UC = Upper Collawash, LC = Lynx Creek, CC = Cougar Creek].

ground-water flow at shallower depths is interrupted by graben-bounding faults and associated topographic divides.

The most conclusive test of the alternative conceptual models would be deep drilling (3–4 km depths) in areas of high heat flow in the Western Cascades. In such areas the lateral-flow model (Fig. 1A) predicts substantially lower heat flow below zones of lateral ground-water flow, whereas the mid-crustal heat-source model (Fig. 1B) predicts relatively minor changes in heat flow with depth. A less expensive (and less conclusive) test is to drill several shallow heat-flow holes in areas where heating due to regional-scale ground-water flow seems unlikely. The U.S. Geological Survey drilled four research holes in 1988–1991 to attempt the latter test.

From north to south, the sites are Fish Creek, Upper Collawash, Lynx Creek and Cougar Creek (Fig. 2). Each site is in an area where relatively high heat flow has been predicted, but the sites are separated from the Quaternary arc by substantial topographic divides and (or) major river valleys that reduce the probability of heating by regional-scale ground-water flow. Local ground-water flow could still affect the thermal field, and near-site hydrology is poorly known; for example, hydraulic head and permeability measurements are lacking. However, the holes were drilled in volcanic and volcaniclastic strata older than 7 Ma (Table 1) that are believed to

Table 1. Lithologic descriptions

Fish Creek site: SE 1/4, sec. 23, T. 5 S., R. 5 E., Wanderers Peak quadrangle. Elevation ~488 m, Road 5420–120 near First Creek crossing, east valley wall of Fish Creek. Drill hole was spudded in landslide deposits, but general area is underlain by ~16 Ma Grande Ronde Basalt of the Columbia River Basalt Group (Anderson, 1978). Lower part of hole penetrated widespread volcaniclastic strata customarily assigned to the Breitenbush Tuff or the Little Butte Formation.

0–85 m:	Homogeneous sequence of basalt flows, probably Columbia River Basalt Group.
85–98 m:	Probably volcanic rock, perhaps lapilli tuff. Might be poorly indurated lithic laharic deposits or lithic-rich distal pyroclastic-flow deposits.
98–101 m:	Dacitic or rhyodacitic moderately welded tuff. Clay altered (probably smectite clays or celadonite). Lithologically similar to most of the Upper Collawash hole.
101–152 m:	Volcaniclastic, probably laharic deposits or a very "muddy" pyroclastic-flow deposit.

Upper Collawash site: Unsectioned, T. 8 S., R. 7 E., Bull of the Woods quadrangle. Elevation ~707 m, at junction of Roads 63 and 6380, west side of Collawash River. Hole penetrated massive tuff that is considered part of the Oligocene and Miocene Breitenbush Tuff.

0–89 m:	Homogeneous dacitic or rhyodacitic, partially to moderately welded tuff, now altered to epidote and celadonite. Reddish variant at 37–40 m is probably local oxidation corresponding to a break between emplacement units.

Lynx Creek site: Unsectioned, T. 12 S., R. 6 E., Coffin Mountain quadrangle. Elevation ~1122 m, end of spur road 1164-537. Drill site is in area mapped as welded pyroxene-bearing ash-flow and air-fall tuff interfingering with andesite and dacite lava, all of middle and late Miocene age (units Tmt and Tma of Black *et al.*, 1987).

0–26 m:	Clastic material (sandstone, laharic deposits?).
26–99 m:	Clay-altered andesitic or dacitic lava flows; at least two flows. Zone at about 82 m contains abundant iron oxide and hydrous iron oxides.
99–105 m:	Less clay-altered, perhaps more silicic lava.

Cougar Creek site: NW 1/4, sec. 17, T. 13 S., R. 6 E., Echo Mountain quadrangle. Elevation ~945 m, Road 2049, north side of Cougar Creek. Drill site is in area mapped as welded pyroxene-bearing ash-flow tuff with fewer epiclastic and air-fall tuff interbeds (unit Tbp of Black *et al.*, 1987). Described as late Oligocene to early Miocene in age, these strata may be as young as middle Miocene on the basis of 13 Ma K–Ar ages from stratigraphically similar beds 18 km north (Laursen and Hammond, 1978).

0–70 m:	Grayish-red, clay-rich rhyodacite (?) lava flow (?) or flows (possible breaks at about 33 and 43 m).
70–143 m:	Volcaniclastic; possibly dacitic ash and crystals; perhaps some reworked as poorly sorted sandstone, some deposited as lahars.

have relatively low average permeability (Blackwell and Baker, 1988, p. 49; Ingebritsen *et al.*, 1992, Table 3). The pre-existing heat-flow data set (Fig. 2) was biased towards hot-spring areas and other topographic lows that represent probable discharge areas for regional ground-water flow from the Quaternary arc.

DRILLING AND COMPLETION HISTORY

The Fish Creek hole (Fig. 2, Table 1) was drilled in the late summer of 1988. The other three holes were drilled in the early summer of 1991. All four holes were drilled by the mud-rotary method. Minimum penetration rates were ~0.3 m/h in the epidote–celadonite tuff of the Upper Collawash hole and the massive silicic lava encountered below 99 m depth in the Lynx Creek hole. Maximum penetration rates were ~15 m/h in the volcaniclastic rocks encountered below 70 m depth in the Cougar Creek hole.

The holes were completed by inserting 2.5 cm inside-diameter PVC or iron-pipe observation tube and filling the annulus with cement grout. Completed depths range from 89 to 150 m. After completion, temperature profiles were measured periodically in order to monitor the return to

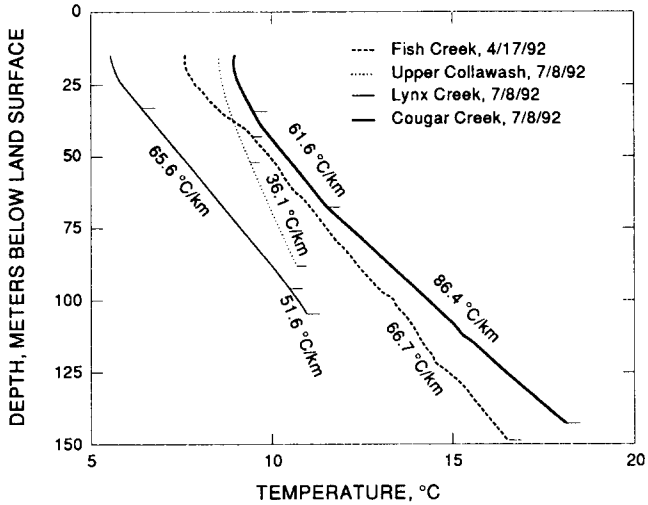

Fig. 3. Near-equilibrium temperature profiles from four holes drilled in the Western Cascades, Oregon. Tick marks indicate depth range across which the temperature gradients were measured.

thermal equilibrium. The near-equilibrium temperature logs shown in Fig. 3 were obtained 1–3 y after completion.

THERMAL CONDUCTIVITY

Grain thermal conductivities (K_g) were measured on cuttings obtained at 3–6 m intervals, using a version of the divided-bar method (Sass *et al.*, 1971). Results of 80 grain-conductivity and grain-density measurements are summarized in Table 2. The harmonic mean grain conductivity of 3.30 W m^{-1} K^{-1} for the epidote–celadonite tuff of the Upper Collawash site is one of the highest values ever reported from the Cascade Range. The other mean grain-conductivity values are in a more typical range of 1.57–1.86 W m^{-1} K^{-1}. Because no core was available, porosity (ϕ) was determined indirectly using bulk-density values (determined by the method of Blake, 1965) from dried outcrop material believed representative of down-hole strata (Table 2). Bulk thermal conductivity (K_b) was estimated using the geometric mean model described by Sass *et al.* (1971) ($K_b = K_g^{1-\phi} K_w^{\phi}$, where K_w, the thermal conductivity of water, $\cong$0.6 W m^{-1} K^{-1}).

TEMPERATURE GRADIENTS

Largely because of the wide variations in thermal conductivity, equilibrium temperature gradients range from 36 to 86°C km^{-1}. The temperature profiles are generally linear below depths of 25–50 m (Fig. 3). However, the gradient changes substantially at depth at two sites: at Lynx Creek, the gradient decreases from 66 to 52°C km^{-1} at a depth of 96 m, and at Cougar Creek the gradient increases from 62 to 86°C km^{-1} at 67 m depth. Both changes in gradient correspond to changes in lithology (Table 1).

Because the holes are relatively shallow and the terrain is steep (Fig. 4), terrain corrections to the measured gradients are commonly large. A two-dimensional numerical algorithm (T. C. Lee, University of California-Riverside, written commun., 1987) was used to obtain terrain

corrections ranging from 2% at Lynx Creek to 35% at the Upper Collawash site. The two-dimensional approximation is fairly good for sites located in the generally linear, v-shaped valleys of the Western Cascades.

Each temperature profile shows vertical gradient changes in the upper 25–50 m (Fig. 3) that are too large to be explained by changes in thermal conductivity. The concavity of the shallow profiles suggests either shallow infiltration of cold ground water or a recent increase in land surface temperature. Extensive post-World War II clearcutting of forest cover in the vicinity of all four drill holes provides a plausible mechanism for surface temperature increases.

UNCERTAINTIES

The uncertainties cited for directly measured rock properties (Table 2: grain conductivity, grain density, bulk density) are standard deviations. The uncertainty in the temperature

Table 2. Thermal-conductivity data

Depth (m)	Grain conductivity (K_g) ($W\ m\ K^{-1}$)	Grain density (ρ_g) ($g\ cm^{-3}$)	Bulk density (ρ_b) ($g\ cm^{-3}$)	Porosity (ϕ) ($1-\rho_b/\rho_g$) —	Bulk conductivity $K_g^{(1-\phi)}K_w^{(\phi)}$ ($W\ m^{-1}\ K^{-1}$)
Fish Creek Site:					
43–152	1.62(0.05)	2.60(0.08)	2.26(0.08)*	0.13(0.06)	1.42(0.12)
n =	18	18	4		
Upper Collawash Site:					
58–89	3.30(0.17)	2.80(0.04)	2.57(0.04)†	0.08(0.03)	3.03(0.28)‡
n =	11	11	3		
Lynx Creek Site:					
34–96	1.57(0.06)	2.44(0.06)	1.70(0.08)§	0.30(0.06)	1.18(0.10)
n =	18	17	7		
96–105	1.63(0.06)	2.50(0.09)	2.50(0.01)	0.02(0.02)	1.60(0.09)
n =	4	4	5		
Cougar Creek Site:					
34–67	1.86(0.23)	2.45(0.06)	—	0.05(0.05)‖	1.76(0.31)
n =	10	10	—		
73–143	1.70(0.10)	2.48(0.09)	1.84(0.07)¶	0.26(0.06)	1.31(0.13)
n =	19	19	3		

*Measured on outcrop samples obtained on Breitenbush Road about 2 km west of Cleator Bend, sec. 24, T. 9 S., R. 6 E. Sampled from moderately bedded, medium-thick beds of blocky-weathering lahars at road level and from overlying very thickly bedded volcaniclastic deposit.

†Measured on outcrop sample from drill site.

‡The lower end porosity value (0.05) was used to calculate the mean bulk conductivity.

§Measured on outcrop samples from Road 1164 on south side of creek crossing, sec. 35, T. 11 S., R. 6 E. Sampled from flow-brecciated andesite lava flow with reddish oxidized top. Samples representative of the 96–105 m depth interval were obtained from the overlying massive andesite flow.

‖No outcrop samples available for bulk-density measurement. Porosity estimated on the basis of lithology.

¶Measured on samples from roadcuts along Highway 20, SE 1/4 sec. 33, T. 13 S., R. 5 E. Grayish, moderately welded plagioclase-phyric ash-flow tuff.

Values for grain conductivity, grain density, and bulk density are mean and standard deviation of measurements. The mean grain conductivity is the harmonic mean (H) of n measurements ($1/H = 1/n[1/a_1 + 1/a_2 + \ldots + 1/n]$). The mean grain and bulk densities are arithmetic means. The uncertainties in the porosity values are the maximum errors obtained using the extremes of the grain- and bulk-density ranges. Similarly, the uncertainties assigned to the bulk-conductivity values were obtained using the extreme values of grain conductivity and porosity.

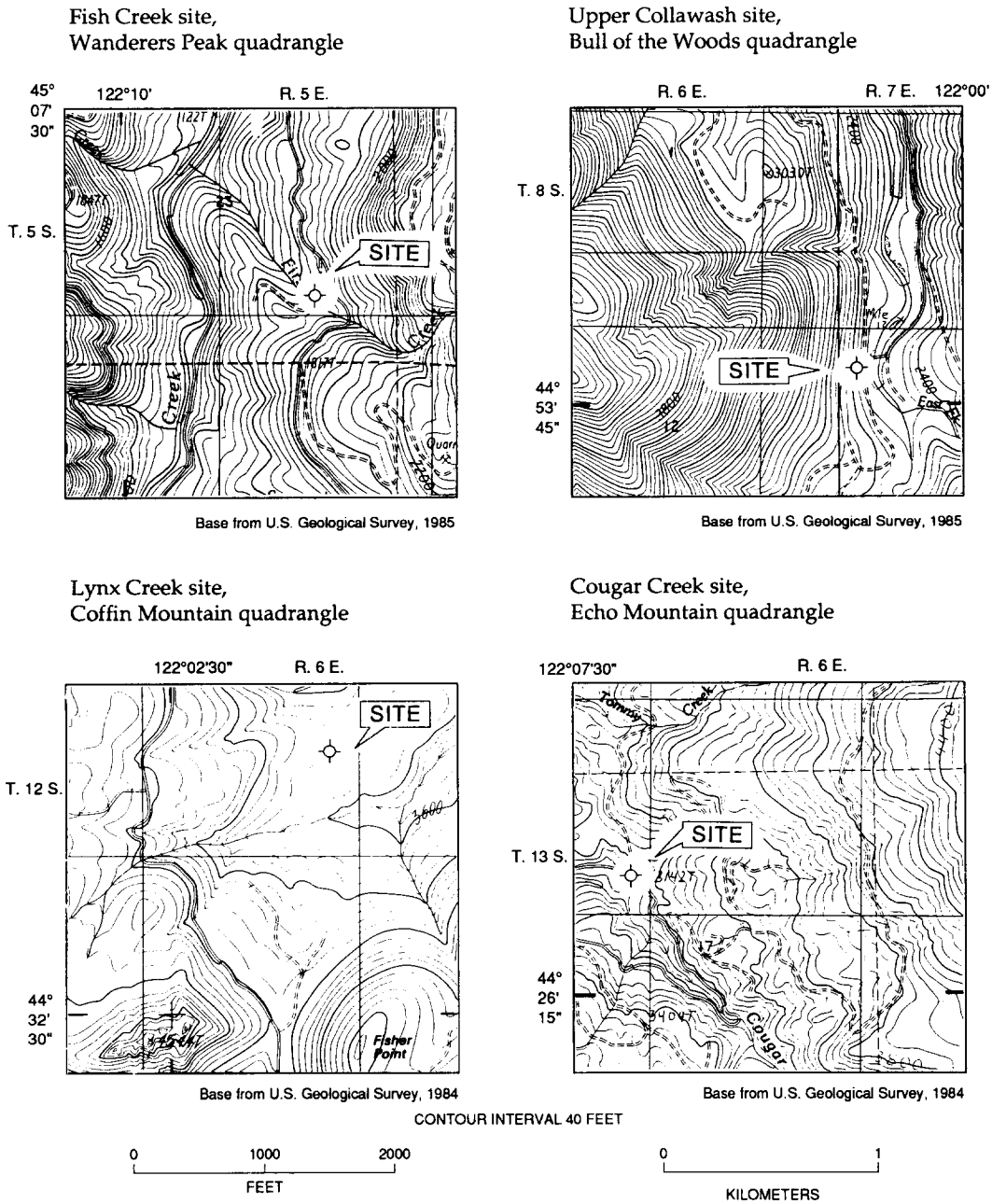

Fig. 4. Maps showing topography in the vicinity of the four new drill holes.

gradient is the standard deviation (S.D.) of the regression coefficient. Uncertainties in porosity, bulk conductivity, and heat flow were calculated as maximum errors using the extreme values (mean − S.D., mean + S.D.) of the relevant parameters. Thus values for all of the quantifiable uncertainties are conservatively large. However, there are additional sources of uncertainty that cannot easily be quantified. These include the correlation of outcrop samples with down-hole strata, which is speculative, and any errors associated with the terrain correction.

HEAT FLOW

Heat-flow estimates for the four drill holes range from 71 to 82 mW m^{-2}, generally somewhat below the values that would be predicted on the basis of previously contoured heat-flow measurements (Fig. 2).

Fish Creek and Upper Collawash sites

At each of these sites the temperature gradient is uniformly linear below an advectively(?) disturbed near-surface zone (Fig. 3), and in each case the outcrop material used for bulk-density measurements was probably representative. Uncertainties in the heat-flow values are $\leq$10% (Table 3).

Lynx Creek site

Here, interpretation is complicated by a change in gradient at 96 m depth (Fig. 3). Such changes are generally related to changes in thermal conductivity and (or) hydrologic flow. The gradient change corresponds roughly to a lithologic change (Table 1) and directly to a major decrease in the drill-penetration rate. The relatively poor correspondence between the change in gradient (96 m) and the reported lithologic change (99 m) may be due to the fact that cuttings were collected only at 3 m intervals, and (or) to the difficulty of assigning exact depths to cuttings samples. Although the contrast in grain conductivity above and below 96 m depth is small, outcrop samples obtained nearby document porosity variations sufficient to explain the change in gradient (Table 2). The upper interval was tentatively correlated with altered, flow-brecciated andesitic lava flows, and the lower interval with an unaltered, massive andesite flow. Estimated heat-flow values for the intervals above and below 96 m are similar (Table 3). They are averaged to obtain the value of 78 mW m^{-2} shown on Fig. 2. The uncertainty is <10%.

Cougar Creek site

This site also has a change in gradient (Fig. 3) that corresponds to a lithologic change (Table 1). At Cougar Creek we did not identify outcrop material clearly representative of the upper interval, and porosity for that interval was estimated from the lithology. The *maximum* possible heat-flow value for the upper (34–67 m) interval is 86 mW m^{-2}; this value assumes zero porosity, so that bulk conductivity is equal to grain conductivity. Heat flow in this interval may be substantially lower if there is significant porosity. The *minimum* likely value for the lower (67–143 m) interval is 79 mW m^{-2}; this value assumes that *in situ* porosity approaches the upper limit of measured outcrop values (0.32). Thus, the feasible estimates for the two intervals overlap in the range of 79–86 mW m^{-2}. We assign a value of 82 mW m^{-2} (Fig. 2), but the uncertainty is >10%, and it is possible that this hole is advectively disturbed by flow at ~67 m depth.

A substantially lower estimate (63 mW m^{-2}) for a shallower hole at the same site was reported previously (Ingebritsen *et al.*, 1991). The previous value was based on a shallow (37–47 m) temperature gradient of 56.6°C km^{-1} (corrected to 42.1°C km^{-1}) and an estimated thermal conductivity of 1.50 W m^{-1} K^{-1}. The deeper hole drilled in 1991 showed a similar gradient (56.4°C km^{-1}) over the same depth interval, but subsequent measurements reported here document substantially larger thermal conductivities.

IMPLICATIONS FOR WESTERN CASCADES HEAT FLOW

The heat-flow maps of Fig. 2 allow comparison between the new measurements and previously published interpretations of Western Cascades heat flow. Though the maps extend

Table 3. Heat-flow estimates

T-R-Sec. 1/4	Name	Longitude (° ′ ″)	Latitude (° ′ ″)	Date (mo/da/yr)	Elevation (m)	Depth (m)	Interval (m)	Gradient Unc. (°C km^{-1})	Gradient Corr. (°C km^{-1})	Cond. (W m^{-1} K^{-1})	Heat flow (mW m^{-2})
5S-5E-23 SE	Fish Creek	122 09 22	45 07 04	4/17/92	488	150	43–150	66.7 (0.3)	51.2	1.41 (0.12)	73 (7)
8S-7E-07 NW	Upper Collawash	122 00 21	44 53 51	7/08/92	707	89	52–89	36.1 (0.1)	23.4	3.03 (0.28)	71 (7)
12S-6E-01 SE	Lynx Creek	122 01 56	44 33 08	7/08/92	1122	105	34–96	65.6 (0.2)	64.3	1.18 (0.10)	76 (7)
							96–105	51.6 (0.4)	50.1	1.60 (0.09)	80 (6)
13S-6E-17 NW	Cougar Creek	122 07 17	44 26 30	7/08/92	945	143	37–67	61.6 (0.8)	46.0	1.76 (0.31)	81 (15)
							67–143	86.4 (0.3)	67.5	1.31 (0.13)	88 (9)

Uncorrected gradients are mean and standard deviation of regression coefficient. Conductivity (Table 2) and heat-flow values are mean and maximum error.

east of the Cascade Range crest, contours there are based on relatively sparse, low-quality data, and both sets of contours are poorly constrained.

These maps rely on similar, overlapping data sets and the differences between them are largely due to differences in the level of generalization. Nevertheless, in some respects they can be viewed as areal representations of the alternate conceptual models of Fig. 1. The relatively detailed contours of Fig. 2A are consistent with the lateral-flow model (Fig. 1A); they show heat-flow highs associated with hot springs and relatively low heat flow between hot-spring groups. The more uniform, generalized contours of Fig. 2B are consistent with a uniform, areally extensive heat source (Fig. 1B).

The contours of Fig. 2A were generated using an inverse-distance-squared weighted average of the nearest data points in each of four quadrants. They indicate estimated conductive heat flow at the depths of most of the measurements (100–200 m). All of the deepest holes in the map area show hydrologically controlled gradient disturbances extending to depths >200 m (Fig. 5), so actual crustal heat flow may be very different from the pattern defined by the shallow (<200 m) measurements. The data used in the contouring were summarized by Ingebritsen *et al.* (1991, pp. 83–91, 192–217). Because the data were interpolated onto a coarse grid (5 × 5 km) and the search radius was large (40 km), the contours do not honor every data point. Nevertheless, the contours represent simple interpolations and extrapolations of data, and are not related to any physical model of a heat source.

Though the contours of Fig. 2B also rely on shallow data, they are intended to represent crustal heat flow and are related to a particular physical model. Where the heat-flow data are sparse, the contours were constrained by a Bouguer gravity gradient, on the basis of an inferred correlation between a negative gravity anomaly and a positive heat-flow anomaly, both attributed to magma accumulation in the mid crust (Blackwell *et al.*, 1982, 1990a). The steepest heat-flow and gravity gradients occur 10–30 km west of the Quaternary arc (Fig. 2B) and define the edge of the proposed mid-crustal heat source (Fig. 1B).

There is a relatively large, systematic inconsistency between the contours of Fig. 2B and the new measurements; all of the new values are lower than those that would be obtained by

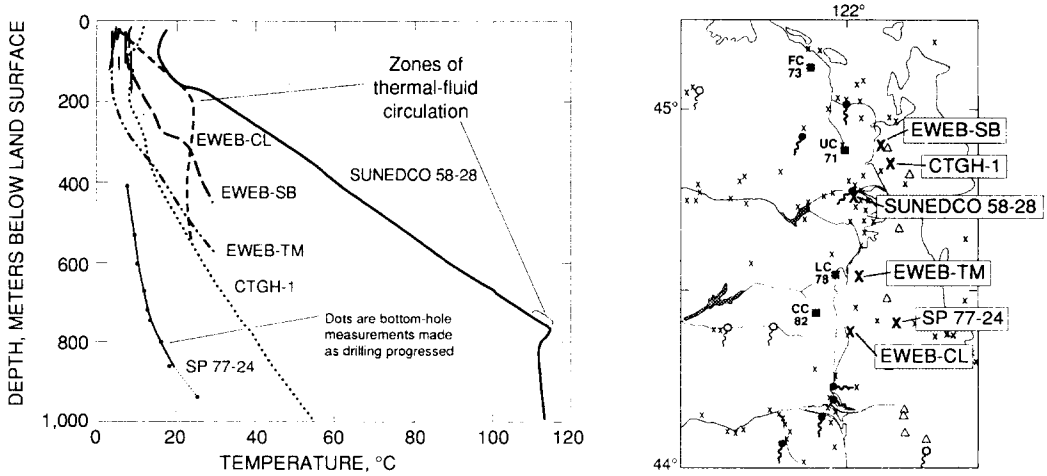

Fig. 5. Temperature–depth profiles from relatively deep (>460 m) drill holes in the study area. The heat-flow contours of Fig. 2A estimate conductive heat flow at depths of 100–200 m; when contouring the heat-flow data, changes in gradient observed at greater depths were ignored. Heat-flow values from EWEB-SB, EWEB-TM, and EWEB-CL were reported by Blackwell *et al.* (1982), CTGH-1 and SUNEDCO 58-28 by Blackwell and Baker (1988) and SP 77-24 by Blackwell (1992).

interpolating between contours. Differences between measured values and values interpolated from Fig. 2B range from a negligible 5 mW m^{-2} (within the error of measurement) at the Cougar Creek site to 20–30 mW m^{-2} at the Upper Collawash and Lynx Creek sites. The difference between the mean measured (76±4 mW m^{-2}) and interpolated (95±7 mW m^{-2}) value is significant.

The contours of Fig. 2A also overestimate heat flow at the Lynx Creek and Upper Collawash sites, but they are approximately correct at the Fish Creek site and *under*estimate heat flow at the Cougar Creek site. The difference between mean measured and interpolated (88±17 mW m^{-2}) values for the four sites is smaller, but still significant.

Figure 6 is a revised heat-flow map modified slightly from Fig. 2A. The only fundamental

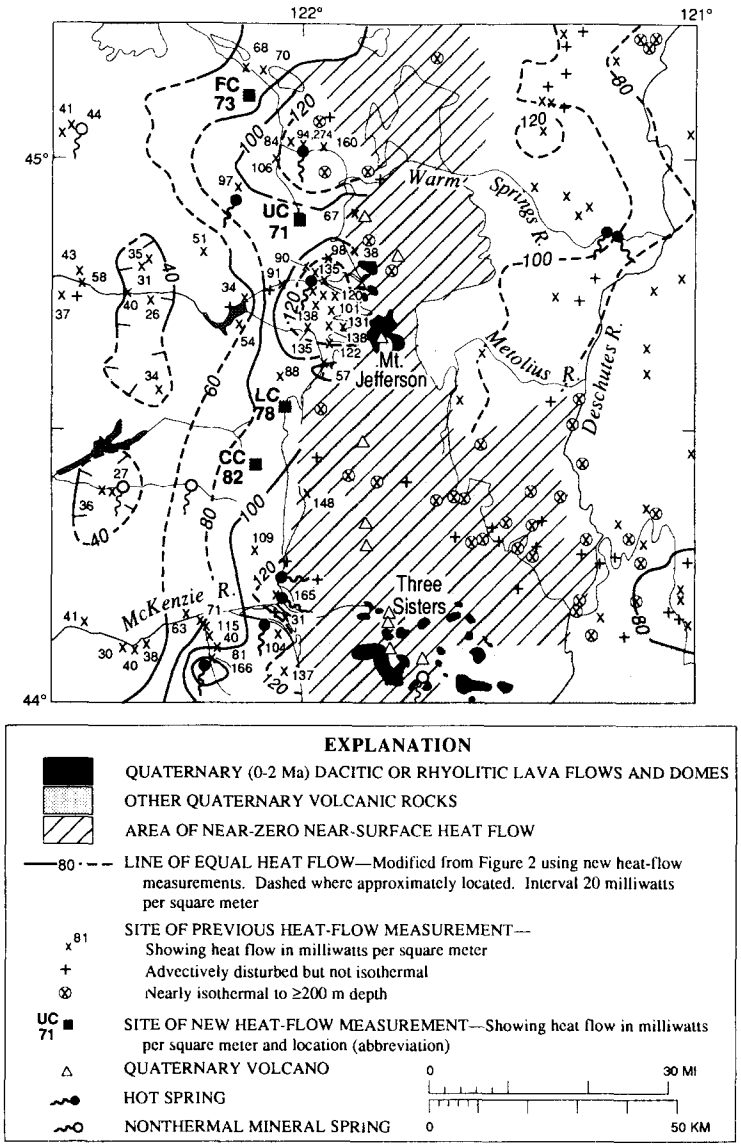

Fig. 6. Revised heat-flow map. See Ingebritsen *et al.* (1991) for information about individual sites.

difference results from the Upper Collawash measurement, which suggests an area of relatively low heat flow between Austin and Breitenbush Hot Springs. Recontouring to accommodate this datum further emphasizes the lobate heat-flow highs around the hot-spring groups. As in the previous map (Fig. 2A), contours were generated by calculating a constrained inverse-distance-squared average of the nearest data points in each of four quadrants.

The data reported here do not conclusively discriminate between the conceptual models of Fig. 1. However, we believe that the inference of relatively low heat flow away from the hot-spring areas tends to support the lateral-flow model.

As noted above, a major argument in support of the existence of a widespread mid-crustal heat source has been an apparent correlation between heat flow and gravity gradients in the Western Cascades (Blackwell *et al.*, 1982, 1990a). A recent analysis of the Western Cascades gravity gradient, using ideal-body theory, indicated that the source of the gravity gradient cannot be deeper than about 2.5 km and is considerably shallower in some locations (Blakely, 1993). It is thus substantially shallower than the proposed mid-crustal heat source (Fig. 1B). Further, the sharpness of the contoured heat-flow transition of Fig. 2B, though relatively poorly constrained, is best matched by a heat source at depths less than 5 km (Blakely, 1993). In the context of the lateral-flow model (Fig. 1A), the shallowness of the causative mass and heat distributions could be explained in terms of lateral flow of heated ground water in relatively shallow, low-density rocks. The explanation in terms of the mid-crustal heat-source model is not obvious.

SUMMARY

Many shallow temperature profiles from the central Oregon Cascade Range are hydrologically disturbed, although they may appear conductive to several hundred meters depth (see, e.g. Fig. 5, EWEB-FC and Sunedco 58-28). Contour maps generated from the generally shallow (100–200 m) heat-flow data set cannot safely be extrapolated much below the depth of measurement. Heat-flow estimates based on deeper data are too sparse to contour, so the actual pattern of crustal heat flow remains unknown. The shallow data set defines lobate heat-flow highs around hot-spring groups in the Western Cascades. Possible geothermal exploration strategies include (1) drilling the relatively well-defined thermal anomalies in the hot-spring areas or (2) "blind" drilling near areas of silicic volcanism in the Quaternary arc. If the lateral-flow model is correct, the source of the thermal anomalies in the hot-spring areas is relatively low-temperature fluid (e.g. Fig. 5, Sunedco 58–28); maximum geothermometer temperatures for the Western Cascade hot springs are <200°C (Mariner *et al.*, 1993). Exploration for thermal anomalies below the near-surface "isothermal" zone in the Quaternary arc will require relatively deep drilling, but anomalies in this area may be related to higher-temperature sources.

Acknowledgements—We thank Ron Baker and Mark Tross for their efforts in drilling and completing the holes, Colin Williams and Jack Kennelly for help with the thermal-conductivity determinations, and Dave Stonestrom for help with the bulk-density measurements. Reviews by Williams, Rick Blakely, Patrick Muffler, Ladislaus Rybach, and Harold Wollenberg improved the manuscript.

REFERENCES

Anderson, J. L. (1978) The stratigraphy and structure of the Columbia River Basalt in the Columbia River drainage. M.S. thesis, Portland State University, Portland, Oregon, 136 pp.

Black, G. L., Woller, N. M. and Ferns, M. L. (1987) *Geologic Map of the Crescent Mountain area, Linn County, Oregon*. Oregon Department of Geology and Mineral Industries Geological Map Series GMS-47, scale 1:62,500.

Blackwell, D. D. (1992) Geothermal and geophysical data from the Santiam Pass 77-24 well. In *Geology and Geothermal Resources of the Santiam Pass Area of the Oregon Cascade Range, Deschutes, Jefferson and Linn*

Counties, Oregon (Edited by Hill, B. E.), pp. 37–52. Oregon Department of Geology and Mineral Industries Open-File Report 0-92-3.

Blackwell, D. D. and Baker, S. L. (1988) Thermal analysis of the Austin and Breitenbush geothermal systems, Western Cascades, Oregon. In *Geology and Geothermal Resources of the Breitenbush–Austin Hot Springs Area, Clackamas and Marion Counties, Oregon* (edited by Sherrod, D. R.), pp. 47–62. Oregon Department of Geology and Mineral Industries Open-File Report 0-88-5.

Blackwell, D. D., Bowen, R. G., Hull, D. A., Riccio, J. and Steele, J. L. (1982) Heat flow, arc volcanism, and subduction in northern Oregon. *J. geophys. Res.* **87**, 8,735–8,754.

Blackwell, D. D. and Steele, J. L. (1985) Heat flow of the Cascade Range. In Guffanti, Marianne, and Muffler, L. J. P., eds., *Proc. Workshop on Geothermal Resources of the Cascade Range. U.S. Geological Survey Open-File Report* 85-521, pp. 20–23.

Blackwell, D. D., Steele, J. L., Frohme, M. K., Murphy, C. F., Priest, G. R. and Black, G. L. (1990a) Heat flow in the Oregon Cascade Range and its correlation with regional gravity, Curie point depths, and geology. *J. geophys. Res.* **95**, 19,475–19,494.

Blackwell, D. D., Steele, J. L., Kelley, S. and Korosec, M. A. (1990b) Heat flow in the State of Washington and Cascade thermal conditions. *J. geophys. Res.* **95**, 19,495–19,516.

Blake, G. R. (1965) Bulk density. In Black, C. A., ed.-in-chief, *Methods of Soil Analysis, Part 1, Physical and mineralogical properties, including statistics of measurement and sampling. Am. Soc. of Agronomy*, Madison, 770 pp.

Blakely, R. J. (1993) Extent of partial melting beneath the Cascade Range, Oregon: Constraints from gravity anomalies and ideal-body theory. Manuscript submitted to *J. geophys. Res.*

Ingebritsen, S. E., Mariner, R. H. and Sherrod, D. R. (1991) Hydrothermal systems of the Cascade Range, north-central Oregon. *U.S. Geol. Surv. Open-File Report* 91-69, 217 p., pending publication as *U.S. Geol. Surv. Professional Paper* 1044-L.

Ingebritsen, S. E., Sherrod, D. R., and Mariner, R. H. (1989) Heat flow and hydrothermal circulation in the Cascade Range, north-central Oregon. *Science* **243**, 1458–1462.

Ingebritsen, S. E., Sherrod, D. R. and Mariner, R. H. (1992) Rates and patterns of groundwater flow in the Cascade Range volcanic arc, and the effect on subsurface temperatures *J. geophys. Res.* **97**, 4599–4627.

Laursen, J. M. and Hammond, P. E. (1978) Summary of radiometric ages of Oregon rocks supplement 1: July 1972 through December 1976. *Isochron/West* No. 23, pp. 3–28.

Mariner, R. H., Presser, T. S. and Evans, W. C. (1993) Geothermometry and water–rock interaction in selected thermal systems in the Cascade Range and Modoc Plateau, western United States. *Geothermics* **22**, 1–15.

Sass, J. H., Lachenbruch, A. H. and Munroe, R. J. (1971) Thermal conductivity of rocks from measurements on fragments and its application to heat-flow determinations. *J. geophys. Res.* **76**, 6376–6414.